

PERFORMANCE OF NANOMETRE-LEVEL RESOLUTION CAVITY BEAM POSITION MONITORS AT ATF2

D. R. Bett, N. Blaskovic Kraljevic, R. M. Bodenstein, T. Bromwich, P. N. Burrows,
 G. B. Christian, C. Perry, R. Ramjiawan, John Adams Institute, Oxford, UK
 S. Araki, A. Aryshev, T. Tauchi, N. Terunuma, KEK, Tsukuba, Ibaraki, Japan
 S. Jang, Dept. of Accelerator Science, Korea University, Sejong, South Korea
 P. Bambade, S. Wallon, LAL, Orsay, France

Abstract

A system of three low-Q cavity beam position monitors (BPMs), installed in the interaction point (IP) region of the Accelerator Test Facility (ATF2) at KEK, has been designed and optimised for nanometre-level beam position resolution. The BPMs are used to provide an input to a low-latency, intra-train beam position feedback system deployed in single-pass, multi-bunch mode with the aim of demonstrating intra-train beam stabilisation on electron bunches of charge ~ 1 nC separated in time by 280 ns. In 2016 the BPM resolution was demonstrated to be below 50 nm using the raw measured vertical positions at the three BPMs. New results will be presented utilising integrated sampling of the raw waveforms, improved BPM alignment and modified cavities to demonstrate a vertical position resolution on the order of 20 nm.

INTRODUCTION

Fast beam-based feedback systems will be required at future single-pass beamlines such as the International Linear Collider (ILC) [1] to maintain high luminosities. For example, at the interaction point (IP), a system operating on nanosecond timescales can correct within a bunch train to steer electron and positron beams into collision. A beam position monitor (BPM) can measure deflections in the outgoing beam and the required correction can be calculated and applied to the other incoming beam via a stripline kicker just upstream.

The Feedback On Nanosecond Timescales (FONT) project [2] has developed feedback correction systems, incorporating digital processors based on Field Programmable Gate Arrays (FPGAs) to achieve beam stabilisation at the KEK Accelerator Test Facility (ATF2) [3]. Demonstration of a feedback system that meets ILC jitter correction and latency requirements is described in [4]. Now the FONT group is working on achieving stabilisation on the nanometre-level at the ATF2 notional IP, where the beam is focused to its smallest vertical size.

In order to reach the required BPM resolution, three low-Q cavity BPMs have been developed, installed and optimised in the ATF2 IP region [5]. The best BPM vertical position resolution measurements the FONT group have achieved using the ATF2 beam will be detailed here. Previous results using these BPMs to drive local feedback can be found in [6,7]. The latest feedback results using one BPM as input to the feedback to stabilise the bunch position to the 50 nm level, and using two BPMs to stabilise to the 40 nm level, are presented in [8].

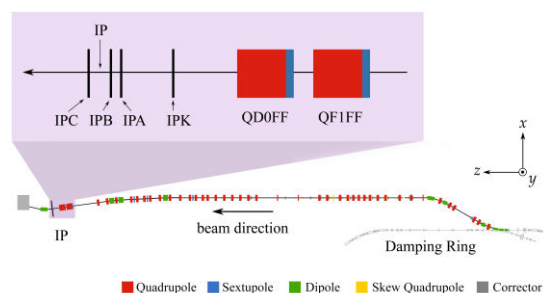


Figure 1: Layout [9] of the ATF2 extraction and final focus beamline with the IP region shown in detail.

EXPERIMENTAL SET-UP

The ATF2 extraction and final focus beamline showing the position of the IP elements is given in Fig. 1. The IP region contains three aluminium C-band cavity BPMs: IPA, IPB and IPC. The BPMs are mounted within the IP vacuum chamber on an x - y mover system, enabling the vertical and lateral position and pitch to be adjusted [10]. Iterative alignment studies have now culminated in a set-up that allows the beam to be steered through the centre of all three BPMs simultaneously. The final focus quadrupoles, QF1FF and QD0FF, can be used to steer the beam by introducing a position offset or to move the beam waist longitudinally by varying the quadrupole strengths. The feedback correction is applied using a stripline kicker.

The original BPMs had lower-than-design loaded Q values and decay times ~ 10 ns. Short decay times reduce the likelihood of signal contamination between pulses when measuring multi-bunch trains, which in typical operation at the ATF2 have a ~ 280 ns separation. However, the very short signal length reduced sensitivity to position offsets. The BPMs were modified to incorporate an indium seal between the cavity body and side covers to raise the loaded Q . Spacers were added under the cavity feedthroughs to reduce external coupling. These modifications increased the decay times to ~ 25 ns to restore the system's position sensitivity. The latest cavity measurements are detailed in Table 1.

Table 1: Measured Cavity BPM Loaded Quality Factors, Q_L , Resonant Dipole Frequencies, f , and Decay Times, τ

BPM	Q_L	f (GHz)	τ (ns)
IPA	1041	6.428	26
IPB	902	6.427	22
IPC	698	6.428	21

Content from this work may be used under the terms of the CC BY 3.0 licence (© 2018). Any distribution of this work must maintain attribution to the author(s), title of the work, publisher, and DOI.

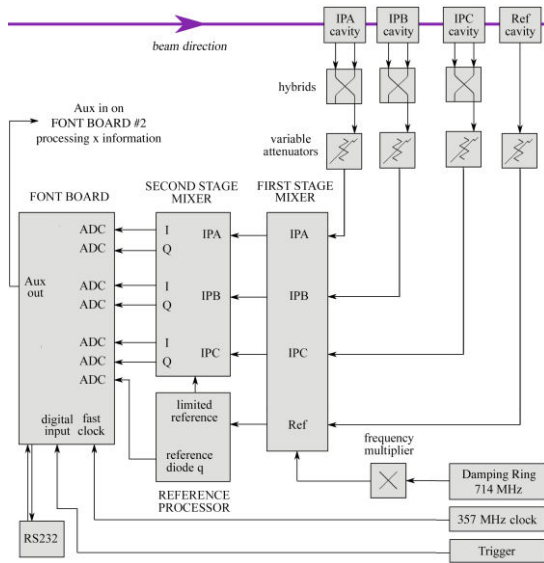


Figure 2: Block diagram of the hardware and processing electronics for the IP cavity BPM y-port signals.

A schematic of the BPM signal processing is given in Fig. 2. Determining the vertical beam position requires the dipole mode y-port signal of the cavity BPMs and the monopole mode of a reference cavity. The cavities were designed so the y-port frequency of both signals is around 6.426 GHz [5]. The signals are down-mixed to baseband using a two-stage down-mixer [11], as follows. The first stage mixer takes the ~ 6.426 GHz reference and dipole signals and mixes each with an external, common 5.712 GHz local oscillator (LO) to produce signals at 714 MHz. The reference is limited and used as an LO to downmix the dipole 714 MHz signals in the second stage mixers, giving two baseband signals: I (dipole and reference mixed in phase) and Q (dipole and reference mixed in quadrature).

The I and Q signals are digitised in a FONT board [12] and normalised by the bunch charge, q , which is deduced from the reference signal amplitude. Example I and Q signals are shown in Fig. 3. They feature a higher-frequency static signal of unknown origin that is bunch charge-dependent. The signals are calibrated against known beam positions (by moving the BPM movers or steering the beam), allowing the vertical beam position to be determined from a combination of I and Q . A duplicate system is used to determine horizontal beam positions.

RESOLUTION METHODS

The vertical position resolution of the three BPMs was measured as follows. First each BPM was calibrated, allowing the position of the beam to be calculated using:

$$I' = I \cos \theta_{IQ} + Q \sin \theta_{IQ}, \quad (1)$$

$$Q' = -I \sin \theta_{IQ} + Q \cos \theta_{IQ}, \quad (2)$$

$$y = \frac{I'}{qk}, \quad (3)$$

where k and θ_{IQ} are constants obtained from calibrating.

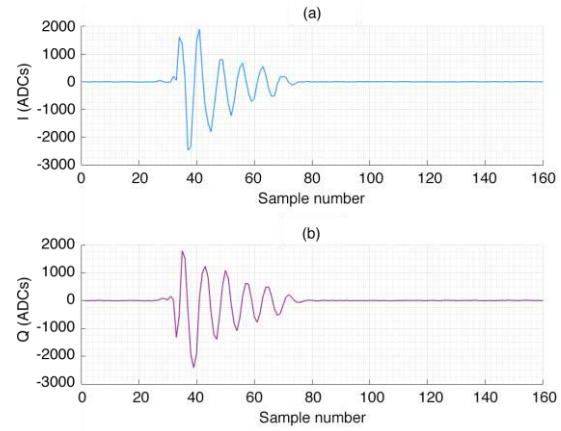


Figure 3: ADC counts versus sample number for a single bunch (a) I signal at IPB (b) Q signal at IPB. The sample separation is 2.8 ns. The data were gathered with a vertical position offset of $\sim 2 \mu\text{m}$ from the electrical centre of IPB.

Secondly, a 2000-pulse data set was taken. For each pulse the beam position measured at two of the BPMs was used to predict the beam position at the third using one of two methods. 1) In the geometric method the position at IPA can be predicted using:

$$y_{IPA} = a_1 y_{IPB} + a_2 y_{IPC}, \quad (4)$$

where a_1 and a_2 are obtained from the beam propagation transfer matrices. 2) In the fitting method, linear regression is performed to find the fit coefficients c_1, c_2, \dots in an equation of the form:

$$I'_{IPA} = c_1 I'_{IPB} + c_2 I'_{IPC} + c_3. \quad (5)$$

Having obtained the fit coefficients, Eq. (5) is used to predict I' values at IPA, which can then be converted to predicted positions using Eq. (3). Additional fit parameters (such as Q' , q , or horizontal I' and Q' values derived using x-port dipole cavity information) can be included in Eq. (5), assuming a linear contribution.

For both methods the residual of the measured and predicted positions at the third BPM is calculated, and the standard deviation δ of the residuals is computed. The resolution, σ , is calculated by scaling δ by the appropriate geometric factor [11], e.g.

$$\sigma = \frac{\delta}{\sqrt{1+a_1^2+a_2^2}}, \quad (6)$$

in the example of positions being predicted at IPA.

RESULTS

Resolution studies were performed in a single-bunch train mode at the ATF2 with 10 dB attenuation on the dipole cavity outputs and at a charge of $\sim 0.5 \times 10^{10}$ electrons per bunch. On using a single sample for I and Q data processing, a sample early in the waveform (Fig. 3) was used, as early samples offer the best signal-to-noise ratio.

Table 2: BPM Vertical Position Resolution Using Geometric and Fitting Methods for a Single Sample of the Digitised Signal and an Integration of 12 Samples

Resolution calculation method	Resolution (nm)	
	Single sampling	Integration
Geometric	49 ± 1	21.5 ± 0.4
Fitting I'	49 ± 1	19.9 ± 0.4
Fitting I', Q'	43 ± 1	19.5 ± 0.4
Fitting I', Q', q	43 ± 1	19.5 ± 0.4
Fitting I', Q', q and x	42 ± 1	19.2 ± 0.4

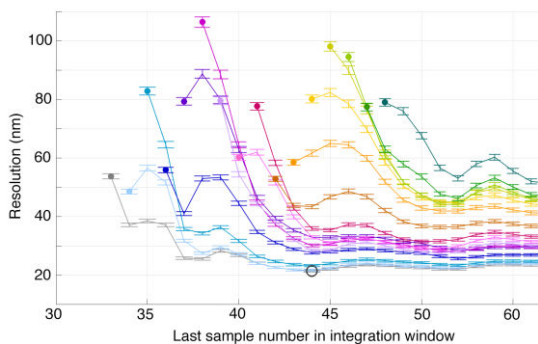


Figure 4: Geometric resolution versus the last sample number in the sampling window. Each colour represents a different starting sample for the integration window, defined by the solid points. The black circle indicates the minimum resolution, 21.5 ± 0.4 nm, found by integrating across 12 samples.

Results of the different resolution estimate methods are presented in the second column of Table 2 using IPA as the prediction BPM. The geometric and I' fitting methods estimate ~ 50 nm resolution. Adding more fit parameters makes a few nanometres improvement, most notably including the quadrature phase Q' . This improvement was found across repeat data sets, suggesting there is residual position information in Q' after the phase rotation and/or that beam conditions have changed between calibrating and data-taking to make the calibration constants invalid.

The unwanted sinusoidal feature in the waveforms (see Fig. 3) complicates identifying optimal sample numbers for best resolution performance. It was therefore of interest to see how resolution varied along the pulse and try an integration method to reduce sample-dependent effects.

Figure 4 shows the geometric resolution for cumulatively increasing integration windows, shifting the starting sample of the integration as well as changing the integration window length. This analysis demonstrates there is always a significant improvement in integrating, with the resolution results using the optimal integration window from Fig. 4 presented in the third column of Table 2. The resolution estimate has been reduced to ~ 20 nm and the results are in good agreement for all analysis methods.

OUTLOOK

The dramatic improvement in resolution estimates using integration, indicate that a modified feedback firmware that enables waveform integration could make a significant improvement to feedback performance. First results with a new integrating firmware can be found in [8].

These best-observed resolution estimates for the ATF2 IP system have not been consistently reproducible, with geometric estimates varying between ~ 20 and ~ 50 nm. Detailed studies demonstrate that most resolution estimates do reduce to ~ 20 nm on applying a fitting method. However, these additional fit parameters cannot be used in a real time feedback system, which for latency reasons can only make use of the raw cavity signals (see Eq. (3)). The geometric method is therefore most representative of the useable resolution for beam stabilisation studies. Future studies will investigate how to ensure this best-resolution geometric performance is repeatable.

CONCLUSIONS

Three low-Q cavity BPMs have been optimised in the ATF2 IP region. Estimates of the BPM resolution were found to have a strong dependence on how the digitised signals were sampled. A resolution of ~ 50 nm was reduced to ~ 20 nm by integrating 12 samples. Additionally, fitting the beam transport and making use of the BPM quadrature-phase signal Q' , bunch charge q , and horizontal BPM signals made only a small improvement in resolution.

ACKNOWLEDGEMENTS

We thank KEK for providing beam time and the ATF2 staff and collaborators for their outstanding support and help. This research was supported by the UK Science and Technology Facilities Council, CERN, and the European Commission's Horizon 2020 Programme through the Marie S.-Curie RISE project E-Jade, Contract No. 645479.

REFERENCES

- [1] C. Adolphsen et al., "The ILC technical design report", volume 3: Accelerator, JAI-2013-001, 2013.
- [2] FONT, <https://groups.physics.ox.ac.uk/font/>
- [3] B. I. Grishanov et al., "ATF2 proposal", vol. 2, KEK Report 2005-9, 2005.
- [4] N. Blaskovic Kraljevic et al., in *Proc. IPAC'16*, paper THPOR034, pp. 3859-3861.
- [5] S. Jang et al., in *Proc. IPAC'16*, paper THOAA02, pp. 3149-3151.
- [6] N. Blaskovic Kraljevic et al., in *Proc. IPAC'16*, paper THPOR035, pp. 3862-3864.
- [7] T. Bromwich et al., in *Proc. IPAC'17*, paper TUPIK112, pp. 1986-1988.
- [8] R. Ramjiawan et al., in *Proc. IPAC'18*, paper WEPAL025.
- [9] G. R. White et al., *Phys. Rev. Lett.*, vol. 112, p. 034802, 2014.
- [10] O. R. Blanco et al., in *Proc. IPAC'15*, paper MOPHA003, pp. 777-780.
- [11] Y. Inoue et al., *Phys. Rev. ST Accel. Beams*, vol. 11, p. 062801, Jun. 2008.
- [12] R. J. ApSimon et al., *Phys. Procedia* 37, p. 2063, 2012.